Zhang *et al. Chem. Biol. Technol. Agric.* (2023) 10:118
https://doi.org/10.1186/s40538-023-00474-9

Chemical and Biological Technologies in Agriculture

RESEARCH

Open Access

Transcriptomic and metabolomic insights into the antimicrobial effect of *Leuconostoc mesenteroides* or lactic acid on pathogenic *Gallibacterium anatis*

Hua Zhang[1,2], HePing HuangFu[3], GuangYong Qin[4], GuoFang Wu[5], Lei Wang[5*] and ZhongFang Tan[4*]

Abstract

Gallibacterium anatis (G. anatis) is an opportunistic poultry pathogen that poses a threat to human health via the food chain and can also lead to great economic losses in poultry industries. Our previous studies have demonstrated that the lactic acid-producing bacteria *Leuconostoc mesenteroides* QZ1178 can effectively inhibit the growth of *G. anatis* by acid production, but the mechanism remains unclear. The aim of the current research was to further investigate the molecular mechanism underlying this acid-induced antimicrobial effect. The TEM results showed that the cell membrane of *G. anatis* (GAC026) was damaged and that cells were lysed in the presence of cell-free supernatants from *Leuconostoc mesenteroides* (CFS) or lactic acid. Lactic acid showed a greater antimicrobial effect than CFS. In this study, the changes in the transcriptome and metabolic profile of *G. anatis* under acid stress at different stages were studied. Using culture medium supplemented with CFS (pH 3.6) or lactic acid (pH 3.6) at a 1:1 ratio, 677 differentially transcribed genes and 374 metabolites were detected in *G. anatis*. The interaction network of all identified differentially expressed genes and metabolites was constructed to outline the regulatory genes and dominant pathways in response to acid stress. The results of real-time reverse transcription quantitative PCR (RT—qPCR) further confirmed the results of the transcriptomic analyses. Typically, succinate, citrate, L-malic acid, and oxaloacetate were reduced by acid stress in *G. anatis*, which suggested that lactic acid greatly disturbed energy metabolism. Overall, this work provides a comprehensive understanding of the stress response and cell death of *G. anatis* caused by lactic acid.

Keywords Lactic acid bacteria, *Leuconostoc mesenteroides*, *Gallibacterium anatis*, Transcriptomic, Metabolomic, Acid stress

*Correspondence:
Lei Wang
wanglei382369@163.com
ZhongFang Tan
tzhongfang@zzu.edu.cn
Full list of author information is available at the end of the article

Graphical Abstract

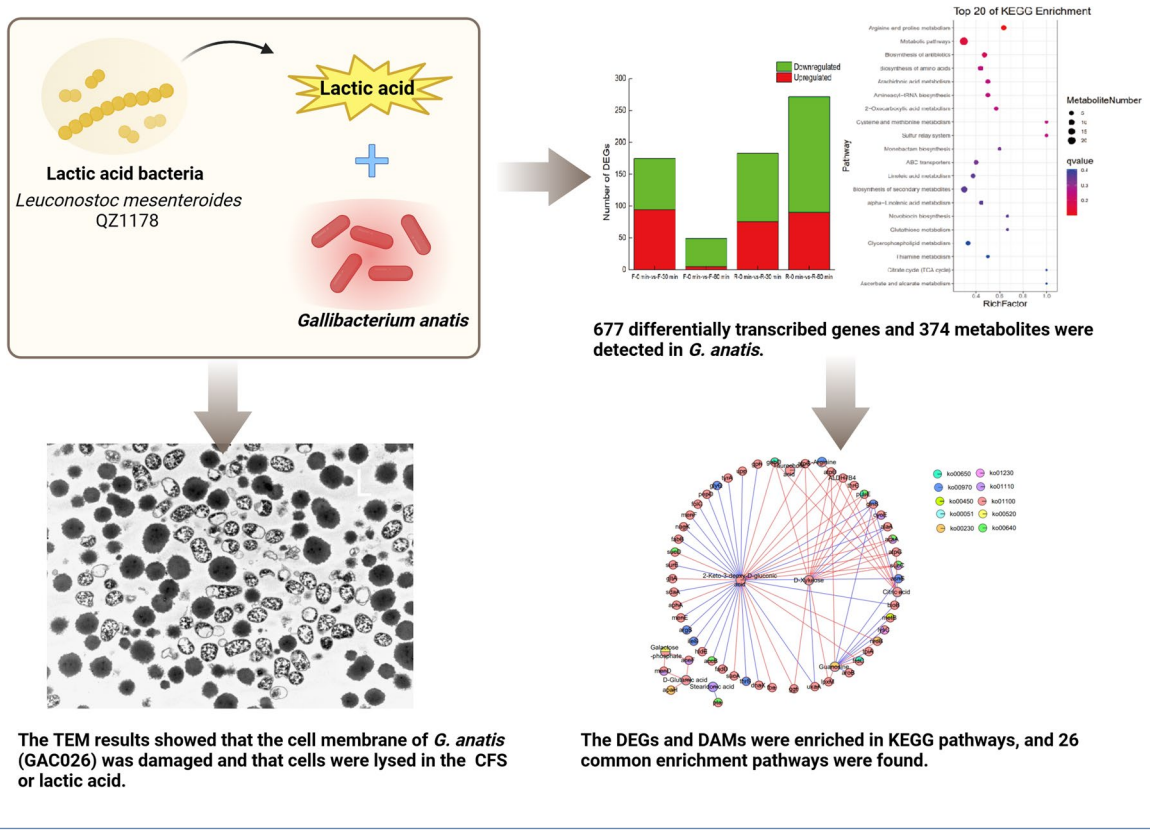

Introduction

Gallibacterium anatis (G. anatis) is an opportunistic pathogen that colonizes the lower genital tract and respiratory tract as part of the normal microbiota of healthy birds [1, 2]. Pathogenic *G. anatis* causes respiratory diseases, salpingitis, and peritonitis in chickens, leading to decreased egg production and increased mortality [3, 4]. *G. anatis* has the ability to infect a wide range of hosts, including domesticated and free-ranging avian animals [5], as well as mammals such as cattle [6] and human beings [7]. Treating this bacterial pathogen with traditional antimicrobial drugs is discouraging owing to the emergence of widespread multidrug resistance [8, 9], whereas the efficacy of classical vaccines is limited due to antigenic diversity [10].

Lactic acid bacteria (LAB) in traditional fermented foods around the world are well known for their probiotic properties [11–13]. The antimicrobial activity of LAB is mainly based on the production of metabolites such as organic acids, hydroperoxide and bacteriocins [14]. Organic acids are toxic to bacterial cells, as they can cause membrane damage and protein misfolding or denaturation [15] and lead to an increase in the intracellular NAD (+)/NADH ratio under low pH conditions [16]. The positive effect of LAB on the balance of animal intestinal microorganisms [17] and the antibiotic-like effects in inhibiting the growth of pathogenic microorganisms found in chickens, pigs, piglets, and cattle have been reported [18–21].

In a previous study, we reported that the fermented solution of *Leuconostoc mesenteroides QZ1178* (*L. m QZ1178*), a type of LAB, effectively inhibited the growth of *G. anatis* by producing acid [22]. However, the in-depth mechanism by which *G. anatis* responds to acid stress is still unknown. In this work, we applied transcriptomic and metabonomic approaches to elucidate the changes involved in the adaptation of *G. anatis* to acid stress conditions. Transcriptomic analysis was conducted using the Illumina sequencing platform followed by validation with real-time qPCR, while metabolomic analysis was completed using positive and negative ion modes. The experimental design is shown in Fig. 1. The current research will contribute greatly to our knowledge about the antimicrobial mechanism of lactic acid bacteria or their acid products against *G. anatis,* which will lay a foundation for the development of new strategies to prevent *G. anatis* infection in domestic animals.

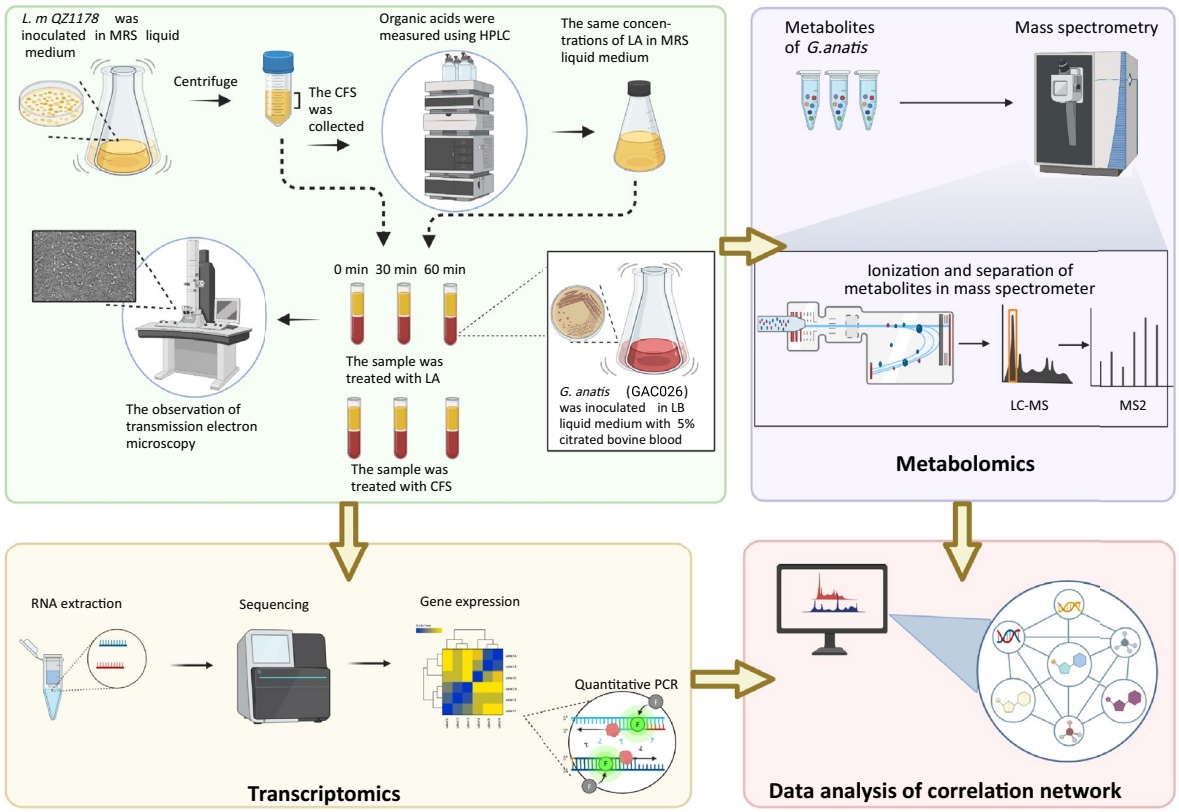

Fig. 1 Experimental design process. Created with BioRender.com

Materials and methods

Bacterial strains and growth conditions

Leuconostoc mesenteroides QZ1178 (*L. m* QZ1178) was previously isolated *from* Qula, a traditional fermented food from Qinghai Province, China. It was maintained in 25% (v/v) glycerol stocks at − 80 °C at the Henan Key Laboratory of Ion-Beam Bioengineering, Zhengzhou University. *L. mesenteroides* QZ1178 was grown in Man Rogosa Sharpe (MRS; Merck, Darmstadt, Germany) solid media at 30 °C for 48 h. The *G. anatis* (GAC026) biovar haemoultica strain was isolated, identified and preserved in the clinical veterinary laboratory of Henan University of Animal Husbandry and Economy [23]. The *G. anatis* strain was cultured on blood agar plates (Bosai Zhengzhou, China) containing brain–heart infusion (Oxoid) agar supplemented with 5% citrated bovine blood in sealed plastic bags at 37 °C.

Bacterial treatment

L. m QZ1178 was inoculated into liquid MRS medium at 30 °C for 24 h. Cultures were centrifuged at 6,000 rpm (4 °C) for 10 min, and the culture fermentation supernatant (CFS) was collected following filtration (0.22 μm membrane). The pH of the supernatant declined sharply and remained at pH 3.6. According to HPLC data, the major organic acid in *L. mesenteroides* QZ1178's CFS was LA, whose concentrations reached 29 mg/ml. The cell suspension was centrifuged at 6,000 rpm (4 °C), and the supernatant was collected. *G. anatis* (GAC026) isolates from chicken palate were selected as the experimental strains. After preculture on solid media, they were inoculated into LB (containing 10% foetal bovine serum) at 37 °C at 180 rpm for 24 h. *G. anatis* (GAC026) was then separated into 10 mL tubes, with each tube containing 4 ml. *L. m.* QZ1178 CFS and LA (29 mg/mL; pH 3.6) were added at 1:1. Experiments were performed in triplicate. For transcriptomic analysis, cell samples were harvested after (treatment time points 0, 30 and 60 min) the addition of CFS or LA. Similarly, samples for metabolomics were collected at 0, 30 and 60 min. Samples for RNA isolation and metabolomic preparation were centrifuged and washed twice with chilled phosphate-buffered saline (PBS). The collected samples were snap-frozen in liquid nitrogen and stored at −80 °C until use.

Transmission electron microscopy

G. anatis (GAC026) was treated with CFS or LA for 60 min. The bacterial samples were fixed in 4% glutaraldehyde at 4 °C overnight. After post-fixation in 1% osmium tetroxide for 1 h, the sections were dehydrated using a graded ethanol series and embedded in resin. An ultramicrotome was used to section the embedded sample blocks, and the sections were then placed on 200-slot grids coated with polyvinyl alcohol ester and imaged using a JEM-1400 electron microscope (JEOL) equipped with an electric coupling camera (Olympus).

RNA isolation, cDNA library construction, and high-throughput Illumina sequencing

Total RNA from the 0 min, 30 min and 60 min samples was isolated using RNeasy Protect Bacteria kits (QIAGEN, USA) according to the manufacturer's instructions. RNA purity and concentration were evaluated by 1% agarose gel electrophoresis. Libraries were constructed using the TruSeq RNASample Prep kit (Illumina, San Diego, CA, USA). High-throughput sequencing was performed on an Illumina Nova6000 platform by Gene Denovo (Guangzhou, China) (http://www.genedenovo.com) [24].

Transcriptome sequencing and enrichment analysis of differentially expressed genes

The raw sequencing data were filtered by fastp (v. 0.18.0) to obtain high-quality clean reads [25]. The rRNA-mapped reads were removed using the Bowtie2 short reads alignment tool (v. 2.2.8), and the remaining clean reads were used in the subsequent assembly and gene abundance calculations [26]. The reference genome of *G. anatis* and the gene annotation files were downloaded from the genome website https://ftp.ncbi.nlm.nih.gov/genomes/refseq/bacteria/Gallibacterium_ anatis/latest_assembly_versions/GCF_000209675.1_ASM20967v1/. All transcripts were obtained with HISAT v. 2.2.4. Differentially expressed genes (DEGs) were identified using DESeq2 to make comparisons between groups [27, 28]. Genes were considered significantly differentially expressed when the P-value was < 0.05 and the fold change was ≥ 2.0 [29]. R (v 3.50 https://www.R-project.org/) was used to conduct correlation analyses of these DEGs. The DEGs were functionally annotated using the KO (KEGG Orthologue) and GO (Gene Ontology) databases.

Validation of gene expression patterns using real-time quantitative PCR

Three biological replicates were prepared for *G. anatis* (GAC026) under CFS or LA conditions (treatment time points 0, 30 and 60 min). Primer 5.0 software (Palo Alto, CA, USA) was used to design RT–qPCR primers. The sequences of all primers are listed in Additional file 1: Table S1. RT–qPCR was performed on the Real-Time PCR Detection System (StepOnePlus, ABI, USA) using cDNA from *G. anatis* (GAC026) at different times after acid stress induction. gyrB was used as a reference gene for RT–qPCR data correction [23].

Metabolomics and bioinformatics analysis

Gene Denovo Biotechnology Co. Ltd. (Guangzhou, China) extracted the primary metabolites from the experimental samples per protocols that have been validated previously [30]. As mentioned previously, there were six biological replications. Each biological replicate was analysed by LC–MS in triplicate.

Targeted metabolomics (energy metabolism)

The metabolomics of bacteria exposed to CFS and LA were analyzed after 60 min of incubation. The three samples from each acid treatment in nutrient broth were evaluated. The extraction procedure was performed by the method published by Bajad et al. [31]. The detection methods were performed as described previously by Cai et al. [32].

Correlation of transcriptomic and metabolomic data

We determined the correlation between DEGs (fold change ≥ 1.5, $P < 0.05$) and differentially accumulated metabolites (DAMs) ($P < 0.05$ and VIP ≥ 1) and utilized the cor function in R to calculate the Pearson correlation coefficient and p-values. The correlation coefficients between genes and metabolites greater than 0.8 were selected for inclusion in a correlation cluster network map. To identify the common pathways, DEGs and DAMs were simultaneously mapped to the KEGG database. Using a coefficient method, the correlation network diagram between genes and metabolites from common KEGG pathways was visualized using Cytoscape software.

Results

The effects of CFS and LA on the morphology of *G. anatis*

Transmission electron microscopy (TEM) was used to observe the ultrastructural changes in *G. anatis* (GAC026) after treatment with CFS or LA. In the control group, the bacteria had a normal shape (Fig. 2A, B). The CFS-treated bacteria were characterized by cell membrane rupture (Fig. C and D). Similarly, the LA-treated bacteria were smaller and had reduced membrane integrity (Fig. E and F). It should be noted that LA was more detrimental to *G. anatis*, as evidenced by the fact that nearly all the cells lost their membranes.

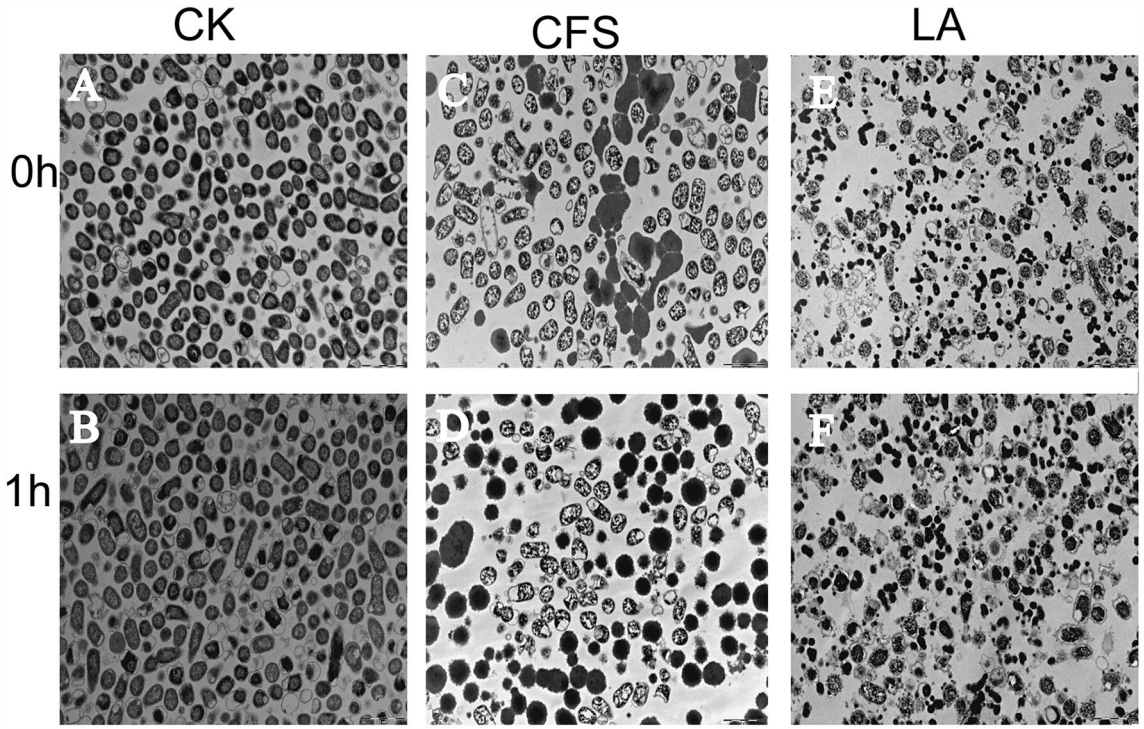

Fig. 2 TEM of *G. anatis* GAC026 treated with CFS or LA. **A** and **B** Normal cells without treatment; **C** and **D** CFS treatment at 29 mg/ml for 0 and 60 min; **E** and **F** LA treatment at 29 mg/ml for 0 and 60 min. Scale bar: 2 μm

The only explanation for this difference was that the CFS content aside from acids was somehow protective to the cells.

Differentially expressed genes of *G. anatis* under acid stress

The effect of acid stress on the GAC026 transcriptome was investigated. Differentially transcribed genes at the mRNA level were evaluated by comparing acid-challenged samples harvested at two time points (30 and 60 min) with those collected at the 0-min time point (set as the control). The transcriptomic data analysis indicated that 1872 genes and 1872 genes at 30 min with CFS and LA, 1876 at 60 min with CFS, 1893 at 60 min with LA, 1874 at 0 min with CFS and 1875 at 0 min with LA were detected (Additional file 1: Table S1). After filtering (≥ 2 fold change, adjusted $p \leq 0.05$), 677 genes were considered significantly differentially expressed (264 up- and 413 downregulated) under acid stress conditions (Additional file 2: Table S2), including 174 at 30 min with CFS (94 up- and 80 downregulated) and 49 at 60 min with CFS (5 up- and 44 downregulated), 183 at 30 min with LA (75 up- and 108 downregulated) and 271 at 60 min with LA (90 up- and 181 downregulated) (Fig. 3A). Taking the F0 min and R0 min samples as the control group, 73 DEGs were identified between F30 min and R30 min (Fig. 3B). However, the number of DEGs was reduced to 17 after 60 min of treatment (Fig. 3C). Consistent with the TEM results, acid stress was the main cause of the antimicrobial effect of CFS within 30 min, while the other components in CFS tended to antagonize this effect by unknown mechanisms.

Gene expression pattern analysis, clustering, and functional enrichment

The genes displayed a considerable difference in expression profiles in response to acid stress for different exposure durations (Fig. 4). The total DEGs at varying exposure times were clustered into different profiles based on the expression patterns of genes using Short Time-series Expression Miner (STEM) software. The most representative clusters were profile 2 and profile 5 in CFS and profile 3 and profile 4 in LA ($p < 0.05$). In profile 2, the expression of 67 gene transcripts decreased and then increased with the increasing duration of CFS treatment (Fig. 4A), and in profile 5, the expression of 126 gene transcripts increased and then decreased with the increasing duration of CFS (Fig. 4B). In profile 3, the expression of 211 gene transcripts remained unchanged and then decreased with the increasing duration of LA (Fig. 4C), and in profile 4, the expression of 101 gene transcripts remained

unchanged and then increased with the increasing duration of LA (Fig. 4D).

To define the functional annotation of the changes during transcription, KO classifications were implemented for the genes in these profiles. As shown in Fig. 4A, the DEGs of profile 2 (gene expression first decreased and then increased under fermentation stress) were mainly enriched in the following KEGG pathways: ribosome, including *rpmH*, *rpmF*, *rplQ*, *rpsD*, *rplX*, *rpsQ*, rpmC, *rplW*, *rplD* and *rplC*; and ABC transporters, including *oppB*, *potC*, *HI_0359*, *xylF*, and *HI_0036* (Additional file 3: Table S3). As shown in Fig. 4B, the DEGs of profile 5 (gene expression first increased and then decreased under fermentation stress) were mainly enriched in the following KEGG pathways: amino sugar and nucleotide sugar metabolism, including *manA*, *manZ*, *manY*, *manX*, *nagA*, *nagE*, *galT*, *nanK* and *nanA*; inositol phosphate metabolism, including *iolB*, *iolA*, *iolG*, *iolE* and *iolD*; phosphotransferase system, including *manZ*, *manY*, *manX*, *fruB*, unknown and *nagE*; and fructose and mannose metabolism, including *manA*, *manZ*, *manY*, *manX*, *fruB* and *fruK* (Additional file 4: Table S4). As shown in Fig. 4C, the DEGs of profile 3 (gene expression remained

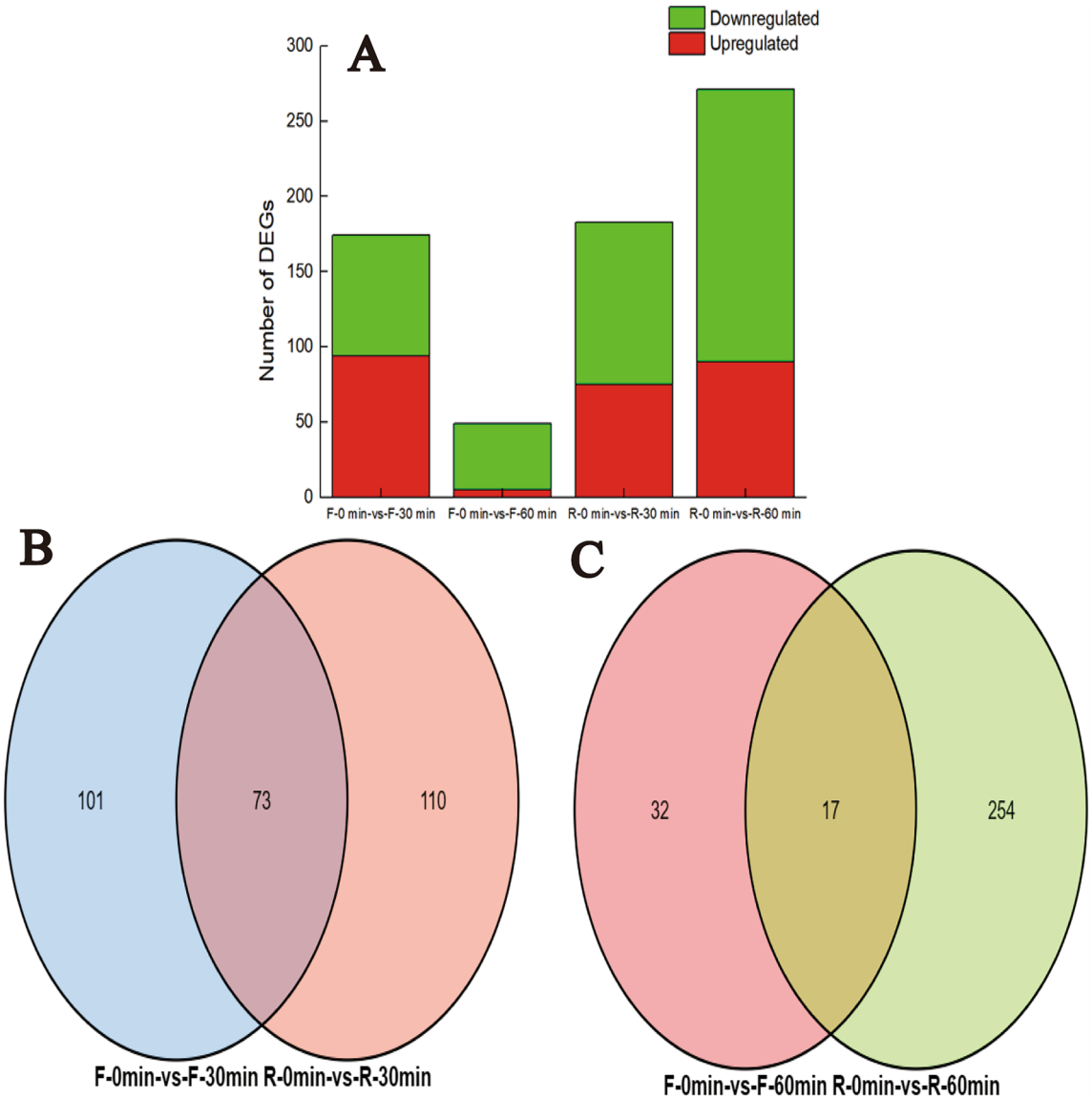

Fig. 3 Differential gene expression after CFS and LA exposure. **A** Regulation of differentially expressed genes (DEGs); **B** and **C** the number of DEGs between samples at the two times is depicted on the Venn diagram. F0 min: 0 min CFS treatment. F30 min: 30 min CFS treatment. F60 min: 60 min CFS treatment. R0 min: 0 min LA treatment. R30 min: 30 min LA treatment. R60 min: 60 min LA treatment

unchanged and then decreased under LA stress) were mainly enriched in the following KEGG pathways: Amino sugar and nucleotide sugar metabolism, including *galE*, *manY*, *manX*, *nagB*, *nagA*, *scrK*, *manB*, *galK*, *galT*, *nanEK* and *nanK*; inositol phosphate metabolism, including *tpiA*, *iolB*, *iolA*, *iolD* and *iolC*; microbial metabolism in diverse environments, including 26 genes; sulfur metabolism, including *dmsC*, *dmsB*, *dmsA*, *ttrB* and *ttrA*; and valine, leucine and isoleucine biosynthesis, including *ilvI*, *ilvE*, *ilvG*, *leuC2* and *alaA* (Additional file 5: Table S5). As shown in Fig. 4D, the DEGs of profile 4 (gene expression remained unchanged and then increased under LA stress) were mainly enriched in the following KEGG pathways: oxidative phosphorylation, including *atpC*, *atpD*, *atpG*, *atpF*, *cyoC*, *cyoD* and *cyoE*; photosynthesis, including *atpC*, *atpD*, *atpG* and *atpF*; propanoate metabolism, including *sucD*, *sucC*, *prpF*, *acnD*, *acsA* and *puuE*; and ribosomes, including *rpmF*, *rplQ*, *rpsD*, *rpmJ*, *rpmD*, *rplX*, *rpmG*, *rplS* and *rpmE* (Additional file 6: Table S6).

The results indicate that the expression levels of most genes related to ribosomes and ABC transporters first decreased and then increased under fermentation stress, but the transcription levels of genes involved in amino sugar and nucleotide sugar metabolism, inositol

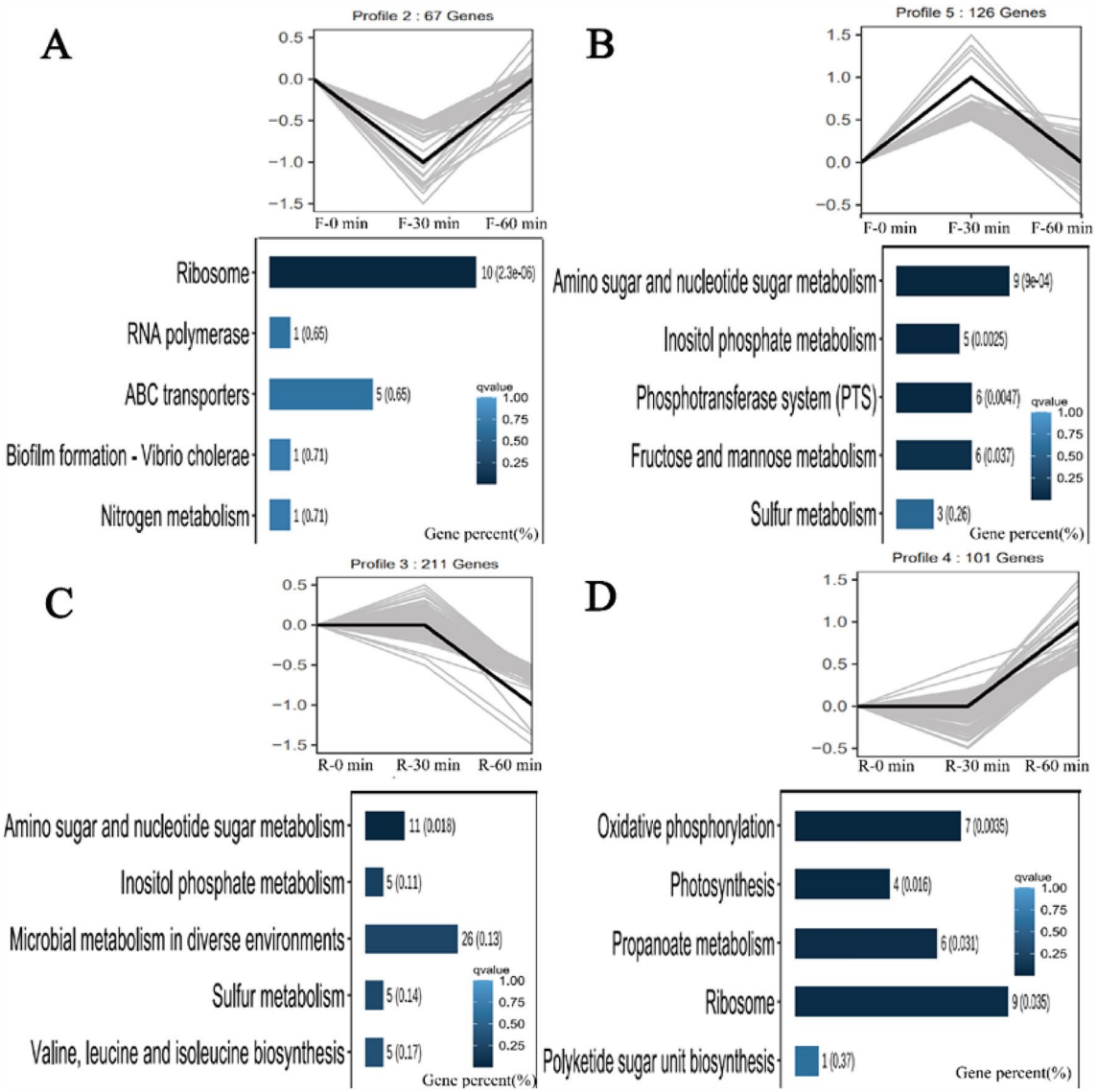

Fig. 4 Patterns of gene expression across two treatments (0 (CK), 30, and 60 min) inferred by STEM analysis; in each frame, the black line represents the expression tendency of all the genes; and the number of genes belonging to each pattern is labelled above the frame. The top five enriched KEGG pathways analysis of profile 2 **A** CFS treatment, profile 5 **B** CFS treatment, profile 3 **C** LA treatment, and profile 4 **D** LA treatment

phosphate metabolism, the phosphotransferase system, fructose and mannose metabolism and sulfur metabolism first increased and then decreased after fermentation. The expression levels of most genes related to amino sugar and nucleotide sugar metabolism, inositol phosphate metabolism, microbial metabolism in diverse environments, sulfur metabolism and valine, leucine and isoleucine biosynthesis remained unchanged and then decreased under LA stress, but the transcription levels of genes involved in oxidative phosphorylation, photosynthesis, propanoate metabolism and ribosomes remained unchanged and then increased after LA exposure. A similar pattern between the gene expression of ribosomes, inositol phosphate metabolism, and amino sugar and nucleotide sugar metabolism, all of which play critical roles in structural integrity and energy balance, was seen with CFS and LA exposure. These results indicated that both CFS and LA inhibit cell growth or cause cell death by disrupting the cell structure, including the membrane, and disturbing energy homeostasis.

qRT–PCR validation of DEGs identified in RNA-Seq analysis

To confirm the reproducibility and accuracy of DEGs identified by RNA-seq analysis, we selected 16 targeted genes (*purM*, *metK*, *copA*, *metN*, *fruK*, *htpG*, *ldh1*, *rplQ*, *rpsS*, *hcp*, *iolA*, *rpoE*, *norB*, *dcuB*, *HI_0227*, and *nanA*) that are involved in structural and energy metabolism for qRT–PCR measurement. The primer sequences for the analyzed genes are shown in Additional file 7: Table S7. In Fig. 5, the gene expression between CFS and LA acid stress-treated *G. anatis* (GAC026) was compared by qRT–PCR and RNA-seq. The fold changes for gene regulation predicted from the transcriptome were verified by qRT–PCR, as both results showed a similar or nearly synchronized pattern.

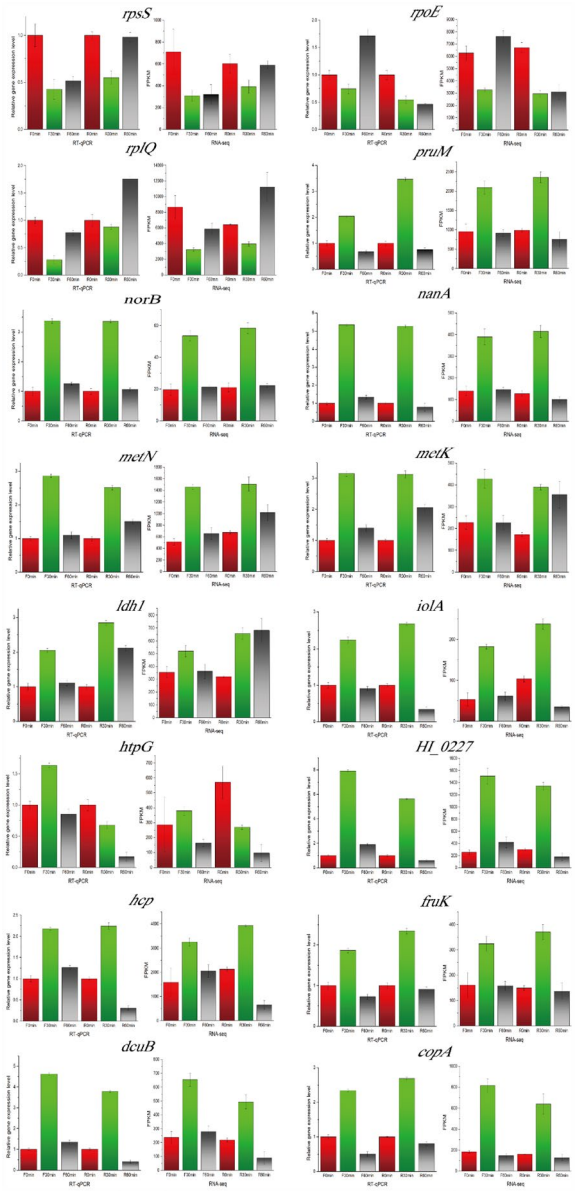

Fig. 5 Comparison of gene expression patterns based on RNA-Seq and qRT—PCR

Nontargeted metabolome analysis and validation of targeted energy metabolites

Nontargeted metabolomic analysis was used for the differential metabolic profiling of *G. anatis* (GAC026) treated with CFS and LA to identify potentially impactful molecules. The CFS- and LA-treated samples were differentiated using orthogonal partial least-squares discriminant analysis (OPLS-DA) (Fig. 6A, B). In total, 374 metabolites were identified (Additional file 8: Table S8). Intracellular metabolites, which were changed significantly under CFS treatment at 60 min, were mainly involved in arachidonic acid metabolism, linoleic acid metabolism, metabolic pathways and alpha-linolenic acid metabolism ($P<0.05$) (Fig. 6C). Intracellular metabolites, which were changed significantly under LA treatment at 60 min, were mainly involved in arginine and proline metabolism, metabolic pathways, biosynthesis of antibiotics, biosynthesis of amino acids, arachidonic acid metabolism, aminoacyl-tRNA biosynthesis, 2-oxocarboxylic acid metabolism, cysteine and methionine metabolism and the sulfur relay system ($P<0.05$) (Fig. 6D). The shared pathways explaining the antimicrobial effect of CFSs under acid stress included the arachidonic acid metabolism and metabolic pathways. In particular, the KEGG pathway (lipid metabolism) mainly involved 7 DAMs upon CFS treatment, namely, PC(16:1(9Z)/18:1(11Z)), PC(16:1(9Z)/P-18:1(11Z)), PC(16:1(9Z)/20:1(11Z)), PC(16:1(9Z)/20:2(11Z,14Z)),

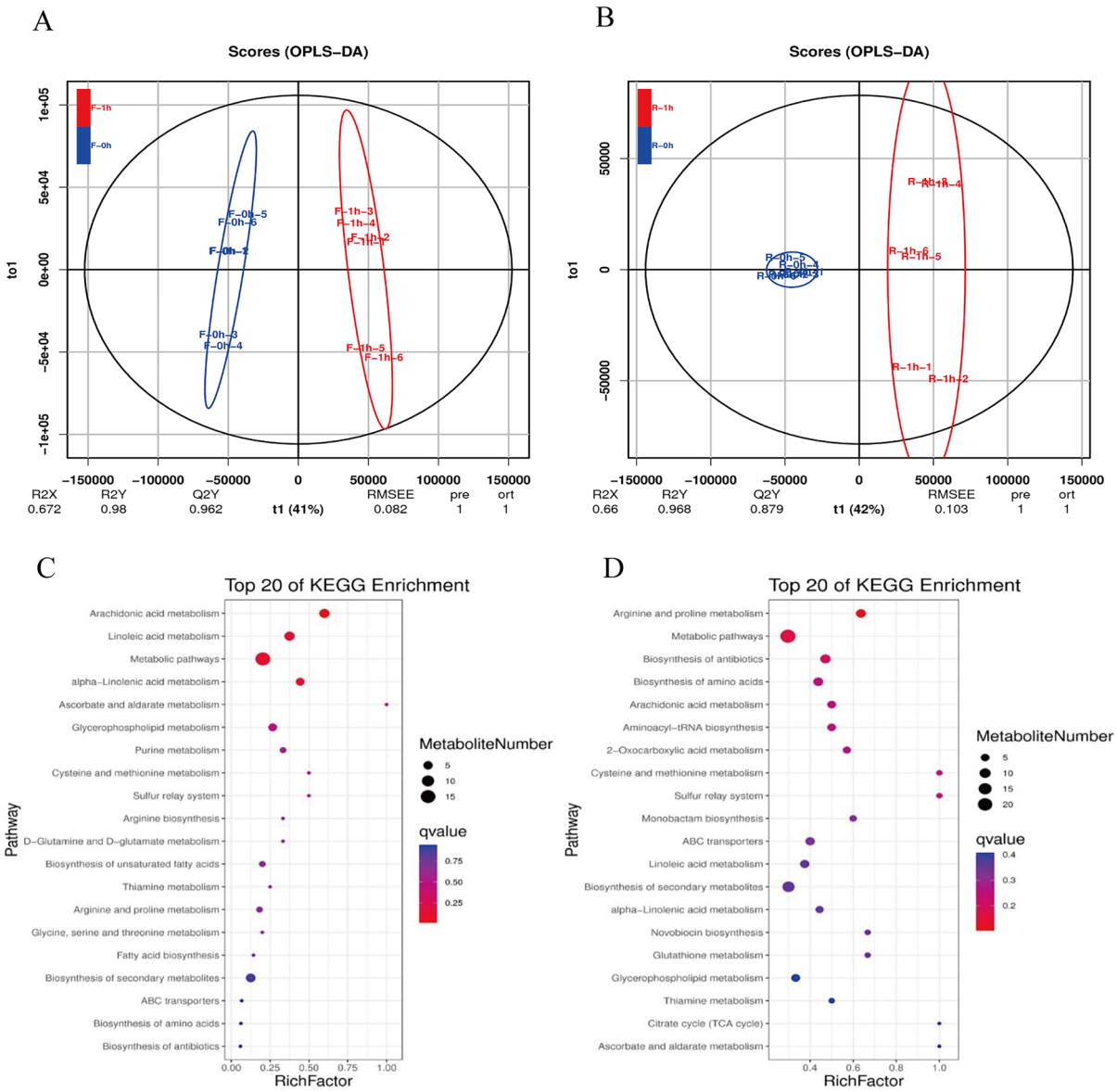

Fig. 6 Nontargeted metabolic profiling of *G. anatis* (GAC026) under acid stress. **A** and **B**, Clustering of orthogonal partial least-squares discriminant analysis (OPLS-DA) for samples treated with CFS and LA, respectively. **C** Bubble plot of KEGG pathways that were significantly different after CFS treatment. **D** Bubble plot of KEGG pathways that were significantly different after LA treatment. $n = 6$ for each group

prostaglandin D2, gamma-linolenic acid and arachidonic acid. The expression of these 7 DAMs was upregulated not only in lipid metabolism but also in metabolic pathways. Additionally, the metabolic pathway contained 8 other DAMs, including 5'-methylthioadenosine (MTA), adenine, adenosine, thiamine, citrulline, D-glutamic acid, creatinine and creatine. Among the DAMs, except for creatine and creatinine, the remaining 6 metabolites were downregulated. The KEGG pathway mainly involved 21 metabolites with LA treatment; L-arginine, L-proline, L-phenylalanine, L-tyrosine and L-isoleucine all increased; 6 DAMs associated with lipid metabolism showed the same change trend as the CFS group; and creatine, creatinine, 2-dehydro-3-deoxy-D-galactonate and pyroglutamic acid were upregulated. However, MTA, adenosine, putrescine, S-adenosylmethionine (SAM), phytosphingosine and thiamine were downregulated. The results suggest that acid stress involves lipid, amino acid and energy metabolism in *G. anatis*. Targeted metabolome analysis confirmed the inhibition of succinate, L-malic acid, oxaloacetate and citrate, which are associated with energy metabolism in the TCA cycle (Fig. 7).

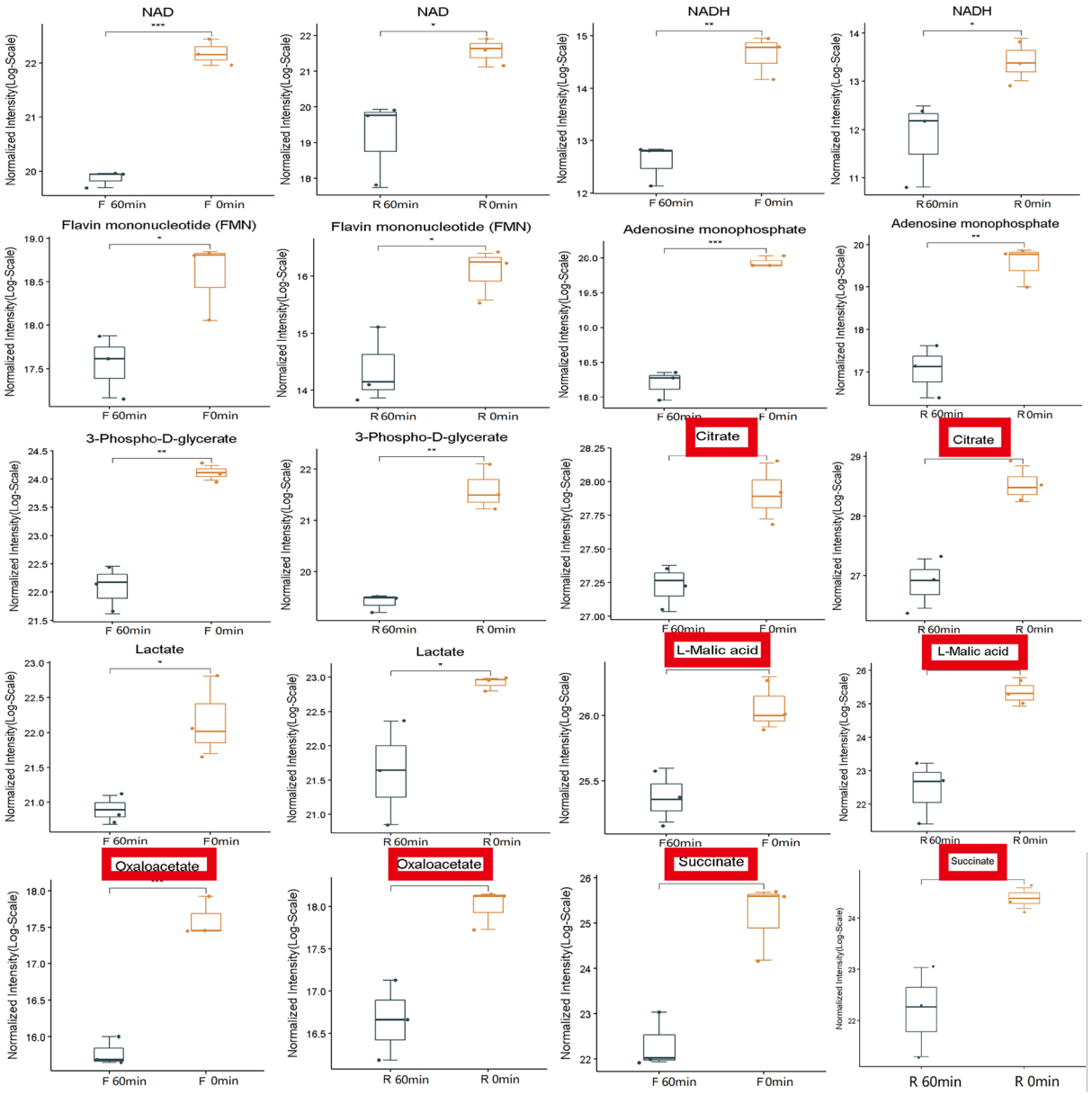

Fig. 7 Targeted metabolic profiling of *G. anatis* (GAC026) under acid stress. Error bars represent the standard deviation of triplicate samples (CK: F 0 min and R 0 min, treatment: F 60 min and R 60 min) (∗∗$p < 0.01$)

Combined analysis of differentially accumulated metabolites (DAMs) and DEGs

To explore the key genes and metabolites that impact to *G. anatis* under acid stress and elucidate the molecular regulatory relationships between them, a combined analysis of metabolomic and transcriptomic data was performed. First, the DEGs and DAMs were enriched in KEGG pathways, and 26 common enrichment pathways were found (Additional file 9: Table S9). The significantly expressed genes and metabolites were primarily associated with the phosphotransferase system (PTS), ascorbate and aldarate metabolism, and purine metabolism following 30 min of treatment with CFS and LA. Conversely, during the 60-min treatment with CFS and LA, they were mainly involved in propanoate metabolism, carbon fixation pathways in prokaryotes, and valine, leucine, and isoleucine degradation. A total of 14 DEGs and 35 DAMs were identified in the purine metabolism pathway, while 7 DEGs and 10 DAMs were associated with propanoate metabolism upon treatment with CFS

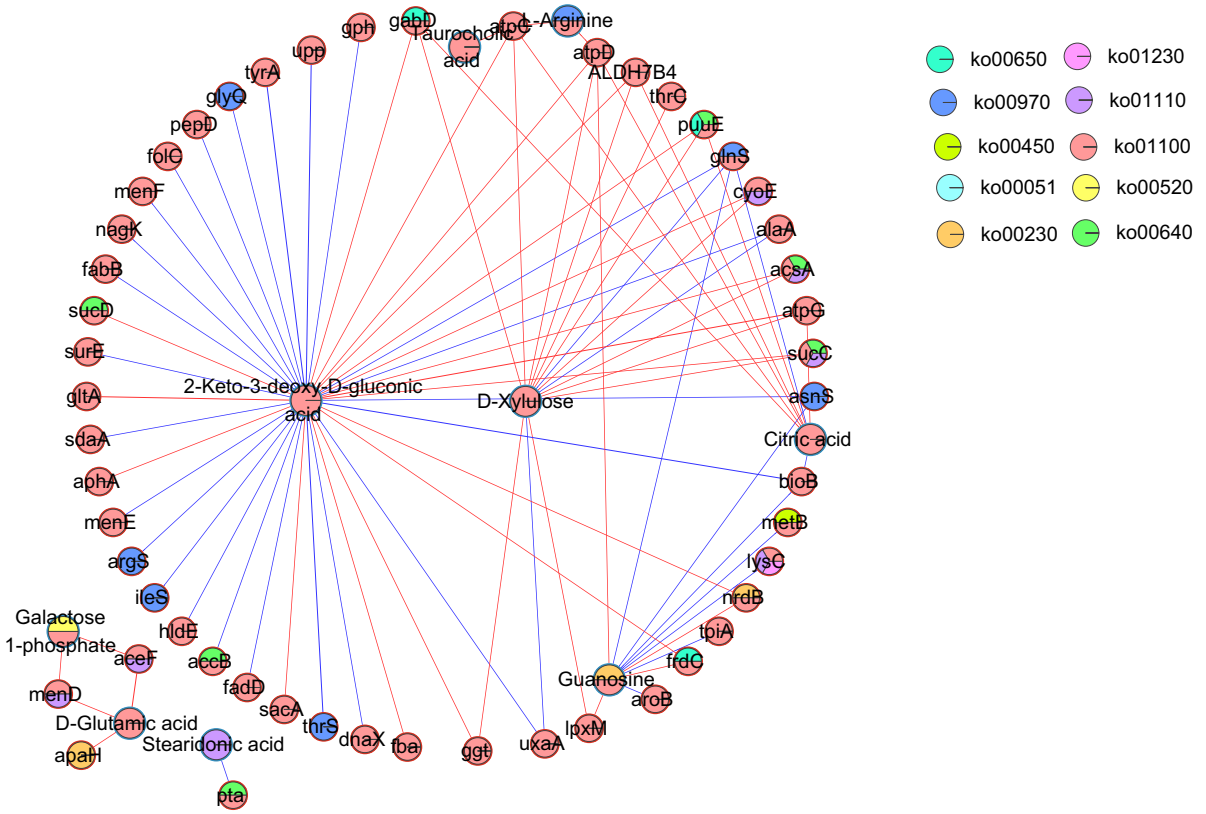

Fig. 8 Pearson's correlation network of the transcript metabolites representing DAMs and DEGs involved in *G. anatis*. The red edges represent positive correlations, while blue edges represent negative correlations. A correlation coefficient > 0.8 was set as the cut-off value. The pie chart on the nodes shows pathways involved in DAM and DEGs. DAMs, differentially accumulated metabolites; DEGs differentially expressed genes

for 60 min. Furthermore, a total of 11 DEGs and 8 DAMs were involved in the fructose and mannose metabolism pathways upon treatment with LA for 30 min, whereas amino sugar and nucleotide sugar metabolism were enriched with 17 DEGs and 18 DAMs after LA treatment for 60 min. Compared with CFS adaptation, the adaptive responses to LA in *G. anatis* cells were more radical and active.

Based on the DAM and DEG data, a subnetwork was constructed for some hub genes to determine transcript–metabolite correlations. Pearson's correlation tests were carried out between relative quantitative changes in metabolites and related transcripts, and we set a correlation coefficient > 0.8 as the cut-off in the analysis. Meanwhile, the pathways involved in DAMs and DEGs are shown in the pie chart. In addition to "metabolic pathways", DAMs and DEGs were also involved in "aminoacyl-tRNA biosynthesis" and "biosynthesis of secondary metabolites" (Fig. 8). These results indicated that the hub genes were highly correlated with their corresponding metabolites. Citric acid, guanosine, D-glutamic acid, L-arginine, taurocholic acid, stearidonic acid, D-xylulose, galactose 1-phosphate and 2-keto-3-deoxy-D-gluconic acid were identified in these biological processes, which reconfirmed the large accumulation of metabolites and their roles during acid stress.

Discussion

The cell membrane plays an important role in controlling the signal transduction of cellular materials, as well as material transport and energy transfer [33, 34]. Organic acids can damage the cells of gram-negative or gram-positive bacteria, destroying their cell surface structure, changing their internal enzyme activity, and altering their biological functions [15, 35]. The antibacterial mechanism of organic acids is partly due to the intracellular pH reduction through the accumulation of ionized forms of the organic acid inside the cytoplasm [36]. In our experiment, *G. anatis* cells tended to shrink under acid stress. A portion of *G. anatis* cells was still viable after exposure to CFS for 60 min, while none of them were culturable, indicating that they were metabolically active yet not culturable. *G. anatis* cells quickly died after exposure to LA. CFS has numerous metabolites, of which LA is the main organic acid that contributes to the acidic environment,

while the others may have different roles. The transcriptional and metabolic profiles reveal some differences in the metabolic changes of *G. anatis* under acid stress.

Nucleotide salvage and purine biosynthesis reactions to acid stress

The assembly of an intact ribosome requires many complex and regulated functions, such as the coordinated synthesis of ribosomal proteins [37]. In this study, some DEGs (*rpmH*, *rpmF*, *rplQ*, *rpsD*, *rplX*, *rpsQ*, *rpmC*, *rplW*, *rplD* and *rplC*) involved in the assembly of ribosome functional components were upregulated at the transcriptional level under acid stress. This might help the bacteria adjust the number of ribosomes in proportion to the metabolic state and the growth rate of cells to meet the demand for protein synthesis under acid stress. Living organisms respond to stressful environmental conditions by redirecting protein synthesis to alleviate cell damage [38]. As a consequence, the transcription of genes involved in cell response and repair is stimulated, while those not involved in those functions, such as genes with roles in cell division machinery, are usually downregulated. In the study by Chueca et al., upregulated genes after carvacrol treatment with available information about their function included purine nucleotides (*purM*) in *Escherichia coli* [39]. Upregulation of *rpmH* under acid stress has also been reported in *Lacticaseibacillus rhamnosus* [40].

Increased expression of genes associated with initiating defence responses

The cellular machineries that maintain redox homeostasis or that function within antioxidant defence systems rely heavily on the regulated reactivities of sulfur atoms either within or derived from the amino acids cysteine and methionine [41]. The ttr operon encoded the tetrathionate response regulatory protein TtrR, the tetrathionate sensor histidine kinase TtrS and three Ttr subunits, TtrC, TtrB and TtrA. The TtrB, TtrC and TtrA proteins could also be involved in arsenic reduction and consequent energy acquisition for bacterial growth in *Leclercia adecarboxylata* [42]. The *ttrRSBCA* gene cluster provides *Escherichia coli* the ability to respire with tetrathionate as an electron acceptor [43]. Transcriptome analysis revealed that the expression of the *ttrB* gene (upregulated by 1.2 fold) and the *ttrC* gene (upregulated by 1.5 fold) was enhanced following treatment with CFS for 30 min. Additionally, the *ttrC* gene (upregulation by 1.3 fold) showed the same trend after LA treatment for 30 min. Transcriptional regulation and organization of the *dcuA* and *dcuB* genes encode homologous anaerobic C4-dicarboxylate transporters in *Escherichia coli* [44]. The C4-dicarboxylate transporters DcuB and DcuC were activated to improve succinate production [45]. After 30 min of acid stress, the expression of the *dcuB* gene was found to be upregulated by 1.7 fold and 1.4 fold in the transcriptomes, respectively. The cells of *G. anatis* survived and adapted to acid stress by activating sulfur metabolism and transporter expression.

The response of genes associated with carbon metabolism to acid stress

The bacterial phosphotransferase system (PTS) is the major transport system for many carbohydrates that are phosphorylated concomitantly with translocation through the membrane (group translocation) [46]. Mannose-6-phosphate isomerase, encoded by the *manA* gene, catalyzes the isomerization of D-mannose and D-fructose and promotes the metabolic uptake of carbon sources [47]. Okochi et al. demonstrated that the overexpression of *manXYZ* in *Escherichia coli* leads to a significant increase in organic solvent tolerance. Transcriptomic analysis revealed a biphasic regulation pattern of *manAXYZ* gene expression following CFS treatment, characterized by initial upregulation followed by subsequent downregulation. The *fruK* gene (1-phosphofructose kinase) and the *fruB* gene (diphosphoryl transfer protein) are implicated in the transport and utilization of fructose [48]. The same trend was also observed during transcription. In extreme alkaline conditions (pH 11), the PTS mannose transport system of *Enterococcus faecalis* undergoes downregulation, while the membrane proteins of *E. faecalis* appear to play a role in redirecting carbohydrate metabolism from the PTS system towards glycerol utilization. Therefore, low expression levels of PTS genes indicate that acid stress reduces carbon source uptake and the energy state.

Signal transduction (inositol phosphate metabolism) in response to acid stress

The role of inositol phosphate metabolism as a coordinator of metabolic adaptability has been recognized; it coordinates the cellular responses to nutrient uptake and utilization from growth factor signalling to energy homeostasis [49]. The *iolABCDEFGHIJ* operon of *Bacillus subtilis* is responsible for myo-inositol catabolism involving multiple stepwise reactions, including the conversion of myo-inositol to an equimolar mixture of dihydroxyacetone phosphate, acetyl-CoA, and CO_2 [50]. Feng et al. proved that downregulation of inositol phosphate metabolism is one of the strategies to adapt to salt stress in *Staphylococcus aureus* [51]. In this study, the *iolB*, *iolA*, *iolG*, *iolE* and *iolD* genes were downregulated with CFS and LA treatment. Inositol

phosphate metabolism is complicated. It involves the conversion of various inositol phosphate molecules, which perform various functions in metabolic pathways. Therefore, we speculated that *G. anatis* reduced the conversion of functional molecules and that downregulated inositol phosphate metabolism to adapt to acid stress.

Increased expression of acid tolerance-related genes

Based on transcriptome data related to acid-stress tolerance in *G. anatis*, it was found that the *puuE* gene (upregulation by 2.2 times) encodes 4-aminobutyrate transaminase. 4-Aminobutanoate (GABA) plays a significant role in micro-organisms in the cytosolic regulation of pH, the control of carbon and nitrogen metabolism, and protection against biotic and abiotic stresses [52, 53]. Yuan et al. demonstrated that the ethanol-stress tolerance of *L. plantarum* WCFS1 was improved by heterologous expression of *puuE* [54]. The expression levels of the *prpF*, *prpC*, and *acnD* genes were upregulated 1.9 times, 2.1 times, and 1.5 times, respectively. According to Tracey et al., in *Shewanella oneidensis* and *Vibrio cholerae*, *prpF* is an accessory protein required to prevent oxidative damage to the Fe/S centre of the active *acnD* enzyme or may be involved in the synthesis or repair of the Fe/S cluster present in *acnD*, and the *acnD* and *prpF* proteins restored the ability to grow on propionate as a source of carbon and energy [55] Differential gene abundance analysis using statistical tests revealed that *G. anatis* cells switched to anaerobic energy metabolism under acid stress conditions, resulting in an increase in propanoate metabolism.

Unsaturated fatty acids levels increased to repair the cell membrane

Microbial fatty acids enable a cell to form membranous components that are essential for its structural integrity. Electron microscopy results revealed that acid stress induced cell membrane rupture in *G. anatis*. Different metabolite enrichment metabolic pathways showed that the contents of PC(16:1(9Z)/18:1(11Z)), PC(16:1(9Z)/P-18:1(11Z)), PC(16:1(9Z)/20:1(11Z)), PC(16:1(9Z)/20:2(11Z,14Z)), prostaglandin D2, gamma-linolenic acid and arachidonic acid were upregulated by CFS and LA treatment at 60 min, which indicated that after being stimulated by acid stress, *G. anatis* synthesized more unsaturated fatty acids to repair the oxidative damage to the cell membrane. This was consistent with previous reports that the ratio of unsaturated fatty acids increased under octanoic acid stress in *E. coli* [56, 57]. Membrane fatty acid adaptation is a common mechanism utilized by bacteria to survive acidic environments [58]. Likewise, genetically engineered *E. coli*, in which trans-unsaturated fatty acids were incorporated into the membrane, led to a significant decrease in membrane fluidity, resulting in high tolerance to carboxylic acids (an organic acid) [59]. However, the induction of fatty acid synthesis or the addition of fatty acids both notably increases membrane leakage and decreases cell viability [57, 60].

Increased biosynthesis of amino acids for pH homeostasis restoration

The arginine system has been identified as an important defence mechanism against damage by acid in several bacteria [61, 62]. Previous reports have proposed that amino acid decarboxylases function to control the pH of the bacterial environment by consuming hydrogen ions as part of the decarboxylation reaction. Examples of this are lysine, arginine, and glutamate decarboxylases, which operate by combining an internalized amino acid (lysine, arginine, or glutamate) with a proton and exchanging the resultant product (cadaverine, agmatine, or γ-aminobutyrate) for another amino acid substrate [63]. As the LA stress time increased, the levels increased by 0.79 times for arginine and 0.78 times for proline. Arginine can also participate in the synthesis of creatine (upregulation by 0.94 fold), which plays an important role in the storage and transfer of phosphate bond energy and ATP synthesis [64]. The metabolism of arginine leads to the production of ornithine, which is subsequently converted into putrescine. In this study, putrescine (downregulated by 2.55 times) is another organic molecule that was important based on its protective role against oxidative damage [65, 66]. A previous study showed that the significantly reduced putrescine levels in nicotine-treated *Pseudomonas sp.* HF-1 could also be associated with resistance to ROS damage from nicotine [67]. In contrast, putrescine plays a necessary role in DNA, RNA and protein biosynthesis [68] and cell division [69].

It was reported that deamination of branched-chain amino acids was one of the mechanisms by which lactic acid bacteria maintain intracellular pH stability [70, 71]. As the LA stress time increased, the levels increased 1.17 times for isoleucine. Aromatic amino acids can protect proteins from bile stress by forming hydrophobic regions [72]. As the LA stress time increased, the levels increased 0.75 times for phenylalanine and 0.83 times for tyrosine. It is hypothesized that aromatic amino acids contribute to resistance to LA stress by forming hydrophobic regions, but the specific mechanism needs to be further explored. We found that the cysteine and methionine metabolic pathways were

significantly altered in the amino acid pathway, including SAM and MTA, which are the primary methyl donors for the methylation of DNA and other macromolecules, including proteins, carbohydrates, lipids, and small molecules such as sterols and nucleosides [73]. SAM and MTA are essential for several metabolic pathways, including biological methylation, polyamine biosynthesis, methionine recycling, and bacterial quorum sensing (QS). Several bacterial behaviours, including virulence factor expression, secondary metabolite production, biofilm formation, motility, and luminescence, are regulated by QS [74, 75], the disruption of which is considered a strategy for controlling virulent pathogens [76, 77]. The data of Bourgeois et al. indicate that disruption of the bacterial methionine metabolism pathway suppresses *S. typhimurium* virulence [78]. The results suggest that amino acid metabolism responds positively to acid stress, with the aim of restoring intracellular pH homeostasis in *G. anatis*. Additionally, it was observed that organic acids can downregulate the expression of virulence factor-related intermediates by inhibiting their production.

Conclusions

This study illustrated the antibacterial effect and partial mechanism of acid treatments (lactic acid and CFS) on *G. anatis* strains. LA and CFS treatment had similar inhibitory effects on *G. anatis* by damaging membrane structure and metabolic pathways. KEGG pathway enrichment analysis showed that these differentially expressed genes were mainly involved in purine metabolism and carbon metabolism, and differentially abundant metabolites were mainly involved in regulating lipids and amino acids. Amino acids and fatty acids increased, and lower concentrations of putrescine, SAM and MTA were detected after treatments. The changes in the target metabolome revealed that the energy metabolism (TCA cycle, glycolysis) and DNA expression and transcription of *G. anatis* were influenced under acid stress. This study provides theoretical support for research on applying LABs or organic acids to control pathogens that may cause food safety issues.

Supplementary Information

The online version contains supplementary material available at https://doi.org/10.1186/s40538-023-00474-9.

Additional file 1: Table S1. Transcriptome sequencing results for CFS and LA.

Additional file 2: Table S2. Differentially significantly expressed genes.

Additional file 3: Table S3. Gene expression first decreased and then increased under fermentation stress.

Additional file 4: Table S4. Gene expression first increased and then decreased under fermentation stress.

Additional file 5: Table S5. Gene expression remained unchanged and then decreased under LA stress.

Additional file 6: Table S6. Gene expression remained unchanged and then increased under LA stress.

Additional file 7: Table S7. Primer sequences for qRT-PCR.

Additional file 8: Table S8. Metabolomics results for CFS and LA.

Additional file 9: Table S9. The combained KEGG enrichment analysis of DAMs and DEGs.

Acknowledgements
Not applicable.

Author contributions
Author contributions HZ is the first author and wrote the paper. HZ and ZT conceived and designed the paper. All authors have read and agreed to the published version of the manuscript.

Funding
This work was supported by the Qing hai Province Key R&D and Transformation Plan of China (No.2023-NK-137).

Availability of data and materials
The datasets used or analyzed during the current study are available from the corresponding author on reasonable request.

Declarations

Ethics approval and consent to participate
Not applicable.

Consent for publication
Written informed consent for publication was obtained from all participants.

Competing interests
The authors declared that they have no competing interest to this work.

Author details
[1]Henan Key Laboratory of Ion-Beam Bioengineering, College of Physics, Zhengzhou University, Zhengzhou, China. [2]School of Food and Biological Engineering, Henan University of Animal Husbandry and Economy, Zhengzhou, China. [3]School of Veterinary Medicine, Henan University of Animal Husbandry and Economy, Zhengzhou, China. [4]School of Agricultural Sciences, Zhengzhou University, Zhengzhou, China. [5]Plateau Livestock Genetic Resources Protection and Innovative Utilization Key Laboratory of Qinghai Province, Key Laboratory of Animal Genetics and Breeding On Tibetan Plateau, Ministry of Agriculture and Rural Affairs, Qinghai Academy of Animal and Veterinary Medicine, Qinghai University, Xining, China.

Received: 12 May 2023 Accepted: 17 September 2023
Published online: 25 October 2023

References

1. Bojesen AM, Torpdahl M, Christensen H, Olsen JE, Bisgaard M. Genetic diversity of *Gallibacterium anatis* isolates from different chicken flocks. J Clin Microbiol. 2003;41:2737–40. https://doi.org/10.1128/JCM.41.6.2737-2740.2003.
2. Bisgaard M, Korczak BM, Busse HJ, Kuhnert P, Bojesen AM, Christensen H. Classification of the taxon 2 and taxon 3 complex of Bisgaard within Gallibacterium and description of Gallibacterium melopsittaci sp. nov., Gallibacterium trehalosifermentans sp. nov. and Gallibacterium salpingitidis sp. nov. Int J Syst Evol Micr. 2009;59:735–44. https://doi.org/10.1099/ijs.0.005694-0.

3. Jordan FTW, Williams NJ, Wattret A, Jones T. Observations on salpingitis, peritonitis and salpingoperitonitis in a layer breeder flock. Vet Rec. 2005;157:573–7. https://doi.org/10.1136/vr.157.19.573.
4. Paudel S, Liebhart D, Hess M, Hess C. Pathogenesis of Gallibacterium in a natural infection model fulfils Koch's postulates: 1. Folliculitis and drop in egg production are the predominant effects in specific pathogen free layers. Avian Pathol. 2014;43:443–9. https://doi.org/10.1080/03079457.2014.955782.
5. Persson G, Bojesen AM. Bacterial determinants of importance in the virulence of *Gallibacterium anatis* in poultry. Vet Res. 2015;46:57–67. https://doi.org/10.1186/s13567-015-0206-z.
6. Van Driessche L, Vanneste K, Bogaerts B, De Keersmaecker SCJ, Roosens NH, Haesebrouck F, De Cremer L, Deprez P, Pardon B, Boyen F. Isolation of drug-resistant *Gallibacterium anatis* from calves with unresponsive bronchopneumonia. Belgium Emerg Infect Dis. 2020;26:721–30. https://doi.org/10.3201/eid2604.190962.
7. Aubin GG, Haloun A, Treilhaud M, Reynaud A, Corvec S. *Gallibacterium anatis* bacteremia in a human. J Clin Microbiol. 2013;51:3897–9. https://doi.org/10.1128/JCM.01638-13.
8. Allahghadry T, Ng DYK, Dibaei A, Bojesen AM. Clonal spread of multi-resistant *Gallibacterium anatis* isolates among Iranian broilers and layers. Vet Res. 2021;52:27–40. https://doi.org/10.1186/s13567-021-00894-1.
9. El-Adawy H, Bocklisch H, Neubauer H, Hafez HM, Hotzel H. Identification, differentiation and antibiotic susceptibility of *Gallibacterium* isolates from diseased poultry. Irish Vet J. 2018;71:5–15. https://doi.org/10.1186/s13620-018-0116-2.
10. Krishnegowda DN, Dhama K, Mariappan AK, Munuswamy P, Yatoo MI, Tiwari R, Karthik K, Bhatt P, Reddy MR. Etiology, epidemiology, pathology, and advances in diagnosis, vaccine development, and treatment of *Gallibacterium anatis* infection in poultry: a review. Vet Q. 2020;40:16–34. https://doi.org/10.1080/01652176.2020.1712495.
11. Mufandaedza J, Viljoen BC, Feresu SB, Gadaga TH. Antimicrobial properties of lactic acid bacteria and yeast-LAB cultures isolated from traditional fermented milk against pathogenic *Escherichia coli* and *Salmonella enteritidis* strains. Int J Food Microbiol. 2006;108:147–52. https://doi.org/10.1016/j.ijfoodmicro.2005.11.005.
12. Adesulu-Dahunsi AT, Jeyaram K, Sanni AI. Probiotic and technological properties of exopolysaccharide producing lactic acid bacteria isolated from cereal-based nigerian fermented food products. Food Control. 2018;92:225–31. https://doi.org/10.1016/j.foodcont.2018.04.062.
13. Toushik SH, Kim K, Ashrafudoulla M, Mizan MFR, Roy PK, Nahar S, Kim Y, Ha SD. Korean kimchi-derived lactic acid bacteria inhibit foodborne pathogenic biofilm growth on seafood and food processing surface materials. Food Control. 2021;129:108276. https://doi.org/10.1016/j.foodcont.2021.108276.
14. Reis JA, Paula AT, Casarotti SN, Penna ALB. Lactic acid bacteria antimicrobial compounds: characteristics and applications. Food Eng Rev. 2012;4:124–40. https://doi.org/10.1007/s12393-012-9051-2.
15. Ning YW, Fu YA, Hou LL, Ma MG, Wang ZX, Li XF, Jia YM. iTRAQ-based quantitative proteomic analysis of synergistic antibacterial mechanism of phenyllactic acid and lactic acid against *Bacillus cereus*. Food Res Int. 2021;139:109562. https://doi.org/10.1016/j.foodres.2020.109562.
16. Ren J, Sang Y, Ni JJ, Tao J, Lu J, Zhao MW, Yao YF. Acetylation regulates survival of *salmonella enterica* serovar typhimurium under acid stress. Appl Environ Microb. 2015;81:5675–82. https://doi.org/10.1128/AEM.01009-15.
17. Gryaznova M, Dvoretskaya Y, Burakova I, Syromyatnikov M, Popov E, Kokina A, Mikhaylov E, Popov V. Dynamics of changes in the gut microbiota of healthy mice fed with lactic acid bacteria and bifidobacteria. Microorganisms. 2022;10:1020. https://doi.org/10.3390/microorganisms10051020.
18. Reuben RC, Roy PC, Sarkar SL, Alam RU, Jahid IK. Isolation, characterization, and assessment of lactic acid bacteria toward their selection as poultry probiotics. BMC Microbiol. 2019;19:253. https://doi.org/10.1186/s12866-019-1626-0.
19. Mo JY, Lu YJ, Jiang S, Yan G, Xing TQ, Xu D, He YY, Xie BK, Lan GQ, Chen BJ, Liang J. Effects of the probiotic, *Lactobacillus delbrueckii* subsp. *bulgaricus*, as a substitute for antibiotics on the gastrointestinal tract microbiota and metabolomics profile of female growing-finishing pigs. Animals. 2022;12:1778. https://doi.org/10.3390/ani12141778.
20. Guerra NP, Bernardez PF, Mendez J, Cachaldora P, Castro LP. Production of four potentially probiotic lactic acid bacteria and their evaluation as feed additives for weaned piglets. Anim Feed Sci Tech. 2007;134:89–107. https://doi.org/10.1016/j.anifeedsci.2006.05.010.
21. Steinberg RS, Silva LCSE, de Souza MR, Reis RB, Bicalho AF, Nunes JPS, Dias AAM, Nicoli JR, Neumann E, Nunes AC. Prospecting of potentially probiotic lactic acid bacteria from bovine mammary ecosystem: imminent partners from bacteriotherapy against bovine mastitis. Int Microbiol. 2021;25:189–206. https://doi.org/10.1007/s10123-021-00209-6.
22. Zhang H, HuangFu HP, Wang X, Zhao SS, Liu Y, Lv HX, Qin GY, Tan ZF. Antibacterial activity of lactic acid producing *L. m QZ1178* against pathogenic *Gallibacterium anatis*. Front Vet Sci. 2021;8:630294. https://doi.org/10.3389/fvets.2021.630294.
23. Huangfu HP, Xu WB, Wang HK, Dong Q, Guo HW, Sun YT, Li YX, Gao WW, Wang WQ, Zhang J, Shi JK, Pan HC, Li CC, Wang LK. Detection of *Gallibacterium anatis* by TaqMan fluorescent quantitative PCR. Avian Pathol. 2018;47:245–52. https://doi.org/10.1080/03079457.2017.1416590.
24. Li X, Ma XD, Cheng YH, Liu JX, Zou JZ, Zhai FF, Sun ZY, Han L. Transcriptomic and metabolomic insights into the adaptive response of Salix viminalis to phenanthrene. Chemosphere. 2021;262:127573. https://doi.org/10.1016/j.chemosphere.2020.127573.
25 Chen SF, Zhou YQ, Chen YR, Gu J. Fastp: an ultra-fast all-in-one FASTQ preprocessor. Bioinformatics. 2018;34:i884ei890. https://doi.org/10.1093/bioinformatics/bty560.
26. Langmead B, Salzberg SL. Fast gapped-read alignment with Bowtie 2. Nat Methods. 2012;9:357–9. https://doi.org/10.1038/NMETH.1923.
27. Love MI, Huber W, Anders S. Moderated estimation of fold change and dispersion for RNA-seq data with DESeq2. Genome Biol. 2014;15:550. https://doi.org/10.1186/s13059-014-0550-8.
28. Robinson MD, McCarthy DJ, Smyth GK. edgeR: a Bioconductor package for differential expression analysis of digital gene expression data. Bioinformatics. 2010;26:139–40. https://doi.org/10.1093/bioinformatics/btp616.
29. Wang LK, Feng ZX, Wang X, Wang XW, Zhang XG. DEGseq: an R package for identifying differentially expressed genes from RNA-seq data. Bioinformatics. 2010;26:136–8. https://doi.org/10.1093/bioinformatics/btp612.
30. Fei F, Bowdish DME, McCarry BE. Comprehensive and simultaneous coverage of lipid and polar metabolites for endogenous cellular metabolomics using HILIC-TOF-MS. Anal Bioanal Chem. 2014;406:3723–33. https://doi.org/10.1007/s00216-014-7797-5.
31. Bajad SU, Lu WY, Kimball EH, Yuan J, Peterson C, Rabinowitz JD. Separation and quantitation of water soluble cellular metabolites by hydrophilic interaction chromatography-tandem mass spectrometry. J Chromatogr A. 2006;1125:76–88. https://doi.org/10.1016/j.chroma.2006.05.019.
32. Cai YP, Weng K, Guo Y, Peng J, Zhu ZJ. An integrated targeted metabolomic platform for high-throughput metabolite profiling and automated data processing. Metabolomics. 2015;11:1575–86. https://doi.org/10.1007/s11306-015-0809-4.
33. Gilbert P, Evans DJ, Evans E, Duguid IG, Brown MRW. Surface characteristics and adhesion of *Escherichia coli* and *Staphylococcus epidermidis*. J Appl Bacteriol. 1991;71:72–7.
34. Wang JB, Qi LL, Mei LH, Wu ZG, Wang HZC. *butyricum* lipoteichoic acid inhibits the inflammatory response andapoptosis in HT-29 cells induced by *Staphylococcus aureus* lipoteichoic acid. Int J Biol Macromol. 2016;88:81–7. https://doi.org/10.1016/j.ijbiomac.2016.03.054.
35. Yung TW, Jonnalagadda S, Balagurunathan B, Zhao H. Transcriptomic analysis of 3-hydroxypropanoic acid stress in *Escherichia coli*. Appl Biochem Biotech. 2016;178:527–43. https://doi.org/10.1007/s12010-015-1892-8.
36. Russell JB, Diez-Gonzalez F. The effects of fermentation acids on bacterial growth. Adv Microb Physiol. 1997;39:205–34.
37. Piersimoni L, Giangrossi M, Marchi P, Brandi A, Gualerzi CO, Pon CL. De novo synthesis and assembly of rRNA into ribosomal subunits during cold acclimation in *Escherichia coli*. J Mol Biol. 2016;428:1558–73. https://doi.org/10.1016/j.jmb.2016.02.026.
38. Harcum SW, Haddadin FT. Global transcriptome response of recombinant Escherichia coli to heat-shock and dual heat-shock recombinant protein induction. J Ind Microbiol Biotechnol. 2006;33:801–14. https://doi.org/10.1007/s10295-006-0122-3.

39. Chueca B, Perez-Saez E, Pagan R, Garcia-Gonzalo D. Global transcriptional response of *Escherichia coli* MG1655 cells exposed to the oxygenated monoterpenes citral and carvacrol. Int J Food Microbiol. 2017;257:49–57. https://doi.org/10.1016/j.ijfoodmicro.2017.06.002.
40. Fan XJ, Zhang KN, Zhang ZC, Zhang Z, Lin X, Liu X, Feng Z, Yi HX. Ribosome profiling reveals genome-wide cellular translational regulation in *Lacticaseibacillus rhamnosus* ATCC 53103 under acid stress. Foods. 2022;11:1411. https://doi.org/10.3390/foods11101411.
41. Miller CG, Schmidt EE. Sulfur metabolism under stress. Antioxid Redox Signal. 2020;33:1158–73. https://doi.org/10.1089/ars.2020.8151.
42. Han YH, Yin DX, Jia MR, Wang SS, Chen YS, Rathinasabapathi B, Chen DL, Ma LQ. Arsenic-resistance mechanisms in bacterium *Leclercia adecarboxylata* strain As3-1: Biochemical and genomic analyses. Sci Total Environ. 2019;690:1178–89. https://doi.org/10.1016/j.scitotenv.2019.07.098.
43. Hensel M, Hinsley AP, Nikolaus T, Sawers G, Berks BC. The genetic basis of tetrathionate respiration in *Salmonella typhimurium*. Mol Microbiol. 1999;32:275–87. https://doi.org/10.1046/j.1365-2958.1999.01345.x.
44. Golby P, Kelly DJ, Guest JR, Andrews SC. Transcriptional regulation and organization of the *dcuA* and *dcuB* genes, encoding homologous anaerobic C4-dicarboxylate transporters in *Escherichia coli*. J Bacteriol. 1998;180:6586–96. https://doi.org/10.1128/JB.180.24.6586-6596.1998.
45. Chen J, Zhu XN, Tan ZG, Xu HT, Tang JL, Xiao DG, Zhang XL. Activating C4-dicarboxylate transporters DcuB and DcuC for improving succinate production. Appl Microbiol Biotechnol. 2014;98:2197–205. https://doi.org/10.1007/s00253-013-5387-7.
46. Lengeler JW, Titgemeyer F, Vogler AP, Wöhrl BM. Structures and homologies of carbohydrate: phosphotransferase system (PTS) proteins. Philos Trans R Soc Lond B Biol Sci. 1990;326:489–504. https://doi.org/10.1098/rstb.1990.0027.
47. Saier MH, Hvorup RN, Barabote RD. Evolution of the bacterial phosphotransferase system: from carriers and enzymes to group translocators. Biochem Soc T. 2005;33:220–4. https://doi.org/10.1042/BST0330220.
48. Kornberg HL. Routes for fructose utilization by *Escherichia coli*. J Mol Microbiol Biotechnol. 2001;3:355–9.
49. Tu-Sekine B, Kim SF. The inositol phosphate system-a coordinator of metabolic adaptability. Int J Mol Sci. 2022;23(12):6747. https://doi.org/10.3390/ijms23126747.
50. Yoshida K, Yamaguchi M, Morinaga T, Kinehara M, Ikeuchi M, Ashida H, Fujita Y. myo-Inositol catabolism in *Bacillus subtilis*. J Biol Chem. 2008;283:10415–24. https://doi.org/10.1074/jbc.M708043200.
51. Feng Y, Gu DZ, Wang ZY, Lu CY, Fan JF, Zhou J, Wang RX, Su XR. Comprehensive evaluation and analysis of the salinity stress response mechanisms based on transcriptome and metabolome of *Staphylococcus aureus*. Arch Microbiol. 2021;204:28. https://doi.org/10.1007/s00203-021-02624-9.
52. Castanie-Cornet MP, Penfound TA, Smith D, Elliott JF, Foster JW. Control of acid resistance in *Escherichia coli*. J Bacteriol. 1999;181:3525–35. https://doi.org/10.1128/JB.181.11.3525-3535.1999.
53. Sanders JW, Leenhouts K, Burghoorn J, Brands JR, Venema G, Kok J. A chloride-inducible acid resistance mechanism in *Lactococcus lactis* and its regulation. Mol Microbiol. 1998;27:299–310. https://doi.org/10.1046/j.1365-2958.1998.00676.x.
54. Yuan L, Zhao HY, Liu LX, Peng S, Li H, Wang H. Heterologous expression of the puuE from *Oenococcus oeni* SD-2a in *Lactobacillus plantarum* WCFS1 improves ethanol tolerance. J Basic Microb. 2019;59:1134–42. https://doi.org/10.1002/jobm.201900339.
55. Grimek TL, Escalante-Semerena JC. The *acnD* genes of *Shewenella oneidensis* and *Vibrio cholerae* encode a new Fe/S-dependent 2-methylcitrate dehydratase enzyme that requires *prpF* function in vivo. J Bacteriol. 2004;186:454–62. https://doi.org/10.1128/JB.186.2.454-462.2004.
56. Royce LA, Liu P, Stebbins MJ, Hanson BC, Jarboe LR. The damaging effects of short chain fatty acids on *Escherichia coli* membranes. Appl Microbiol Biot. 2013;97:8317–27. https://doi.org/10.1007/s00253-013-5113-5.
57. Royce LA, Yoon JM, Chen YX, Rickenbach E, Shanks JV, Jarboe LR. Evolution for exogenous octanoic acid tolerance improves carboxylic acid production and membrane integrity. Metab Eng. 2015;29:180–8. https://doi.org/10.1016/j.ymben.2015.03.014.
58. Fozo EM, Kajfasz JK, Quivey RG Jr. Low pH-induced membrane fatty acid alterations in oral bacteria. FEMS Microbiol Lett. 2004;238:291–5. https://doi.org/10.1016/j.femsle.2004.07.047.
59. Tan ZG, Yoon JM, Nielsen DR, Shanks JV, Jarboe LR. Membrane engineering via trans unsaturated fatty acids production improves *Escherichia coli* robustness and production of biorenewables. Metab Eng. 2016;35:105–13. https://doi.org/10.1016/j.ymben.2016.02.004.
60. Lennen RM, Kruziki MA, Kumar K, Zinkel RA, Burnum KE, Lipton MS, Hoover SW, Ranatunga DR, Wittkopp TM, Marner WD, Pfleger BF. Membrane stresses induced by overproduction of free fatty acids in *Escherichia coli*. Appl Environ Microb. 2011;77:8114–28. https://doi.org/10.1128/AEM.05421-11.
61. Liu YP, Tang HZ, Lin ZL, Xu P. Mechanisms of acid tolerance in bacteria and prospects in biotechnology and bioremediation. Biotechnol Adv. 2015;33:1484–92. https://doi.org/10.1016/j.biotechadv.2015.06.001.
62. Shabayek S, Spellerberg B. Acid stress response mechanisms of Group B Streptococci. Front Cell Infect Mi. 2017;7:395. https://doi.org/10.3389/fcimb.2017.00395.
63 Cotter PD, Hill C. Surviving the acid test: responses of gram-positive bacteria to low pH. Microbiol Mol Biol Rev. 2003;67:429–53. https://doi.org/10.1128/MMBR.67.3.429-453.2003.
64. Sundekilde UK, Rasmussen MK, Young JF, Bertram HC. High resolution magic angle spinning NMR spectroscopy reveals that pectoralis muscle dystrophy in chicken is associated with reduced muscle content of anserine and carnosine. Food Chem. 2017;217:151–4. https://doi.org/10.1016/j.foodchem.2016.08.104.
65. Tkachenko AG, Nesterova LY, Pshenichnov MP. Role of putrescine in the regulation of the expression of the oxidative stress defense genes of *Escherichia coli*. Microbiology. 2001;70:133–7. https://doi.org/10.1023/A:1010365110538.
66. Pirintsos SA, Kotzabasis K, Loppi S. Polyamine production in lichens under metal pollution stress. J Atmos Chem. 2004;49:303–15. https://doi.org/10.1007/s10874-004-1239-2.
67. Ye YF, Wang X, Zhang LM, Lu ZM, Yan XJ. Unraveling the concentration-dependent metabolic response of *Pseudomonas sp*. HF-1 to nicotine stress by 1H NMR-based metabolomics. Ecotoxicology. 2012;21:1314–24. https://doi.org/10.1007/s10646-012-0885-4.
68. Tabor CW, Tabor H. Polyamines in microorganisms. Microbiol Rev. 1985;49:81–99. https://doi.org/10.1128/MMBR.49.1.81-99.1985.
69. Gutierrez-Rios RM, Freyre-Gonzalez JA, Resendis O, Collado-Vides J, Saier M, Gosset G. Identification of regulatory network topological units coordinating the genome-wide transcriptional response to glucose in *Escherichia coli*. BMC Microbiol. 2007;7:53–71. https://doi.org/10.1186/1471-2180-7-53.
70. Sanchez B, Champomier-Verges MC, Collado MD, Anglade P, Baraige F, Sanz Y, Reyes-Gavilan CGDL, Margolles A, Zagorec M. Low-pH adaptation and the acid tolerance response of *Bifdobacterium longum* biotype longum. Appl Environ Microb. 2007;73:6450–9. https://doi.org/10.1128/AEM.00886-07.
71. Len MCL, Harty DWS, Jacques NA. Proteome analysis of *Streptococcus mutans* metabolic phenotype during acid tolerance. Microbiology. 2004;150:1353–66. https://doi.org/10.1099/mic.0.26888-0.
72. Lv LX, Yan R, Shi HY, Shi D, Fang DQ, Jiang HY, Wu WR, Guo FF, Jiang XW, Gu SL, Chen YB, Yao J, Li LJ. Integrated transcriptomic and proteomic analysis of the bile stress response in probiotic *Lactobacillus salivarius* LI01. J Proteomics. 2017;150:216–29. https://doi.org/10.1016/j.jprot.2016.08.021.
73. Parveen N, Cornell KA. Methylthioadenosine/S-adenosylhomocysteine nucleosidase, a critical enzyme for bacterial metabolism. Mol Microbiol. 2011;79:7–20. https://doi.org/10.1111/j.1365-2958.2010.07455.x.
74. Antunes LCM, Ferreira RBR, Buckner MMC, Finlay BB. Quorum sensing in bacterial virulence. Microbiol-Sgm. 2010;156:2271–82. https://doi.org/10.1099/mic.0.038794-0.
75. LaSarre B, Federle MJ. Exploiting quorum sensing to confuse bacterial pathogens. Microbiol Mol Biol R. 2013;77:73–111. https://doi.org/10.1128/MMBR.00046-12.
76. Hentzer M, Wu H, Andersen JB, Riedel K, Rasmussen TB, Bagge N, Kumar N, Schembri MA, Song ZJ, Kristoffersen P, Manefield M, Costerton JW, Molin S, Eberl L, Steinberg P, Kjelleberg S, Hoiby N, Givskov M. Attenuation of *Pseudomonas aeruginosa* virulence by quorum-sensing inhibitors. EMBO J. 2003;22:3803–15. https://doi.org/10.1093/emboj/cdg366.
77. Smith RS, Iglewski BH. *Pseudomonas aeruginosa* quorum sensing as a potential antimicrobial target. J Clin Invest. 2003;112:1460–5. https://doi.org/10.1172/JCI200320364.

78. Bourgeois JS, Zhou DG, Thurston TLM, Gilchrist JJ, Ko DC. Methylthioadenosine suppresses salmonella virulence. Infect Immun. 2018;86:e00429-e518. https://doi.org/10.1128/IAI.00429-18.

Publisher's Note